JOURNAL OF GEOPHYSICAL RESEARCH, VOL. 97, NO. D7, PAGES 7613–7617, MAY 20, 1992

Interpretation of Seasonal Cloud-Climate Interactions Using Earth Radiation Budget Experiment Data

R. D. CESS,[1] E. F. HARRISON,[2] P. MINNIS,[2] B. R. BARKSTROM,[2] V. RAMANATHAN,[3] AND T. Y. KWON[1]

This investigation proposes an approach for using satellite radiation budget data to interpret and understand seasonal cloud-climate interactions in a manner that can serve as one means of testing and improving numerical climate models. By employing Earth Radiation Budget Experiment data it is demonstrated that, relative to the annual-mean climate, seasonal cloud variations produce radiative heating of the surface-atmosphere system in the summer hemisphere, together with cooling in the winter hemisphere. It is further illustrated that this is an integrated effect resulting from the combination of seasonal variations in cloud amount, cloud vertical distribution, and cloud optical depth.

1. INTRODUCTION

Three-dimensional general circulation models (GCMs) are the most comprehensive numerical climate models for projecting climate change caused by increasing concentrations of greenhouse gases. However, a roughly threefold disagreement in one measure of climate sensitivity exists among 19 atmospheric GCMs [*Cess et al.*, 1989, 1990], and this is caused by significant intermodel differences in climate-induced changes of cloud-radiative forcing, i.e., cloud feedback. Clearly, there is a need to improve our understanding of cloud-climate interactions. Although it does not serve as an analog for long-term climate change, seasonal variations of cloud-radiative forcing constitute one means of testing GCMs and, perhaps more importantly, of providing physical insights into cloud-climate interactions.

In this study we employ Earth Radiation Budget Experiment (ERBE) satellite data to evaluate, for the first time, seasonal cloud-climate interactions as manifested by seasonal variations of cloud-radiative forcing. Relative to the annual-mean climate, seasonal cloud variations are found to produce radiative heating of the surface-atmosphere system in the summer hemisphere and cooling in the winter hemisphere. It is further demonstrated that this hemispheric radiative heating/cooling is an integrated effect caused not only by seasonal changes in cloud amount but also by seasonal variations of cloud vertical distribution and cloud optical depth. The key point is that recently available measurements of cloud-radiative forcing provide unique insights for understanding seasonal cloud-climate interactions.

2. SEASONAL CLOUD-RADIATIVE FORCING

The term cloudy is used to denote a domain containing both overcast-sky and clear-sky regions, as in the work by *Ramanathan et al.* [1989], while the term clear refers to an average of clear-sky regions within that domain. We employ monthly-mean top-of-the-atmosphere (TOA) reflected shortwave (SW) and emitted longwave (LW) radiative fluxes as provided by the ERBE for 2.5° longitude by 2.5° latitude grids and for both cloudy and clear designations [*Ramanathan et al.*, 1989; *Harrison et al.*, 1990]. By separately averaging clear-sky measurements the ERBE provides radiation budget data that, in addition to conventional cloudy measurements, refer to a "clear-sky" Earth having the same climate as with clouds present.

With H representing the net TOA radiative heating of the climate system, then

$$H = (1 - \alpha)S - F \tag{1}$$

where α, S, and F, respectively, denote the albedo, solar irradiance, and emitted LW radiation at the TOA. For present purposes CRF* will be used to denote the conventional definition of cloud-radiative forcing, so that [*Ramanathan et al.*, 1989]

$$\text{CRF}^* = H - H_c = (F_c - F) - S(\alpha - \alpha_c) \tag{2}$$

where the subscript c is used for clear-sky quantities. Positive values of ΔCRF* indicate that clouds radiatively heat the climate system while negative values correspond to cooling. Since $F_c - F$ is generally positive, this represents the greenhouse warming caused by clouds; the opposite effect caused by reflection of SW radiation will cool the system. On a global average the solar cooling dominates so that CRF* is negative [*Ramanathan et al.*, 1989; *Harrison et al.*, 1990].

The present goal is to investigate the seasonal variation of cloud-radiative forcing. Letting Δ denote the seasonal perturbation of a given quantity about its annual-mean value, while an overbar is used to denote the annual-mean quantity (e.g., $\Delta S = S - \bar{S}$), it follows from (1) and (2) that

$$\Delta\text{CRF}^* = (\bar{\alpha}_c - \bar{\alpha})\Delta S + (\Delta\alpha_c - \Delta\alpha)S + (\Delta F_c - \Delta F) \tag{3}$$

In deriving the above it is important to note that by definition $\overline{\alpha S} = \bar{\alpha}\,\bar{S}$, because it is the flux that is being averaged. The first term in (3) is related solely to seasonal variability of the solar irradiance and thus contains no information concerning seasonal cloud-climate interactions. To isolate the requisite cloud-climate interactions, we delete this term and define the seasonal change in cloud-radiative forcing as

[1]Institute for Terrestrial and Planetary Atmospheres, State University of New York, Stony Brook.
[2]Atmospheric Sciences Division, NASA Langley Research Center, Hampton, Virginia.
[3]Scripps Institution of Oceanography and California Space Institute, University of California at San Diego, La Jolla.

Paper number 92JD00547.
0148-0227/92/92JD-00547$05.00

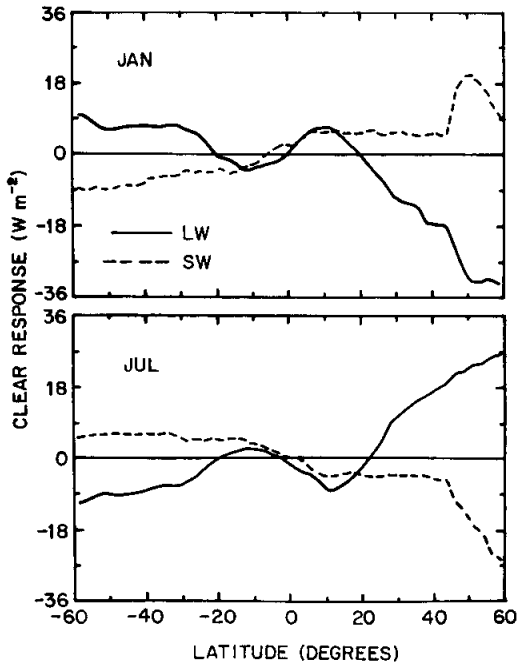

Fig. 1. Zonal-mean LW and SW components of the clear radiative response ΔR_c for (upper panel) January and (lower panel) July.

$$\Delta\text{CRF} = (\Delta\alpha_c - \Delta\alpha)S + (\Delta F_c - \Delta F) \quad (4)$$

It is important to recognize that ΔCRF, and not ΔCRF*, properly portrays the effects of seasonal cloudiness variations on the TOA radiation budget. In the present context of monthly-mean data, ΔF and $\Delta\alpha$ denote monthly-mean departures from the annual mean, while S is the monthly-mean solar irradiance.

For later purposes it will prove instructive to recast (4) as

$$\Delta\text{CRF} = \Delta R_c - \Delta R \quad (5)$$

where

$$\Delta R = S\Delta\alpha + \Delta F \quad (6)$$

Physically, ΔR and ΔR_c represent the change in net upward TOA radiation and thus represent the radiative responses of the climate system to seasonal climate change.

If we were to choose the domain to be the entire globe and if we were considering a change from one equilibrium climate to another, in contrast to seasonal climate change, then one could define and interpret global climate feedback mechanisms. *Cess et al.* [1989, 1990], for example, have shown that cloud feedback is directly related to global-mean ΔCRF and that it so acts to either amplify (positive feedback) or damp (negative feedback) climate change. It was intermodel variations in global-mean ΔCRF that produced the threefold variation in one measure of climate sensitivity among the 19 GCMs [*Cess et al.*, 1989, 1990]. It is important to distinguish here between CRF and ΔCRF. The fact that the global-mean CRF is negative [*Ramanathan et al.*, 1989] does not imply that cloud feedback is negative, since the feedback is related to ΔCRF. In fact, 15 of the 19 GCMs produced positive ΔCRF and negative CRF, so that for these models global warming resulted in less cloud cooling, that is, positive cloud feedback. In that the present study refers to seasonal change it is not possible to address cloud feedback. Nevertheless, the seasonal ERBE data provide useful information concerning mechanisms that contribute to the seasonal ΔCRF as we now demonstrate.

3. ERBE RESULTS

As previously discussed, monthly-mean ERBE data are used for 2.5° longitude by 2.5° latitude grids. These data were obtained by instruments on two satellites: ERBS that has a 57° (relative to the equator) inclined orbit, and National Oceanic and Atmospheric Administration (NOAA) 9 which is in a Sun-synchronous orbit with an 0230 equator crossing time. We restrict attention to latitudes less than 60° because of difficulties in distinguishing between clear and overcast regions at high latitudes [*Ramanathan et al.*, 1989; *Harrison et al.*, 1990], in addition to the fact that there is a sampling discontinuity at roughly 60° latitude as a result of the ERBS orbit. Four months of ERBE data (April, July, October, 1985; January 1986), as reported by *Harrison et al.* [1990], have been used in the present study. A problem with ERBE data, as well as with GCMs, is missing clear-sky data [*Harrison et al.*, 1990] which must be filled through interpolation, and so we based our annual means on only four months to minimize the amount of interpolation. The missing clear-sky data is the result of persistent cloud cover over some regions throughout a month. Recently, *Randall and Tjemkes* [1991] have used the full 12 months of data and found results similar to ours.

3.1. *Seasonal Response*

To place seasonal ΔCRF results in perspective, we first employ the ERBE data to illustrate seasonal radiative responses. The ERBE data provide useful insights into the clear-sky response ΔR_c, for which the LW and SW components are shown in Figure 2 for January and July; we first

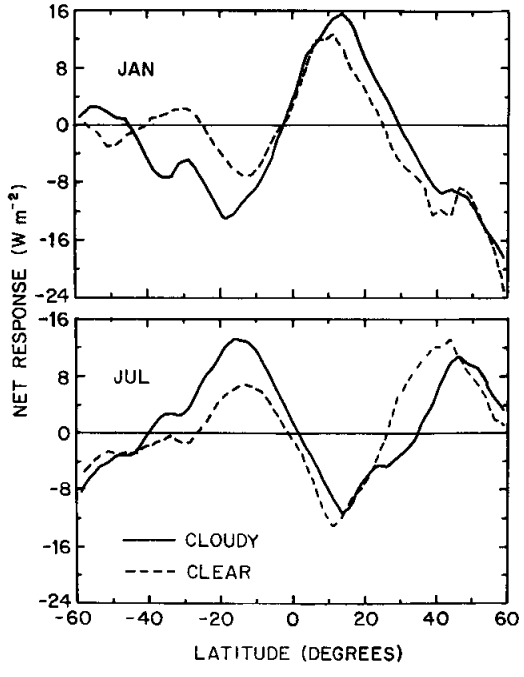

Fig. 2. Zonal-mean clear and cloudy net radiative responses ΔR_c and ΔR for (upper panel) January and (lower panel) July.

discuss July. The enhanced LW clear response in the northern hemisphere (NH) mid-latitudes (Figure 1, lower panel) is due to the warm (relative to the annual mean) mid-latitudes in July producing enhanced TOA emission. The magnitude of the reverse effect in the southern hemisphere (SH) is less because the greater SH ocean expanse results in less seasonal climate variation. The LW response in the tropics is caused by quite a different mechanism. Here the seasonal change in surface temperature is minimal, while there is a substantial increase in tropical NH atmospheric water vapor (and a related SH reduction) due to the migration of the intertropical convergence zone (ITCZ) into the summer hemisphere. Because water vapor is a greenhouse gas, it acts to reduce LW TOA emission, and this change in atmospheric water vapor explains the related variation in tropical LW clear response (Figure 1, lower panel).

The July SW response is negative in the NH and positive in the SH (Figure 1, lower panel) due largely to the seasonal variation of the solar zenith angle. Since the TOA albedo increases with increasing solar zenith angle, this by itself causes reduced SW reflection (and thus reduced SW response) in the summer hemisphere and the reverse in the winter hemisphere. The effect is amplified at high NH latitudes where diminished snow/ice cover in July (relative to the annual mean) further reduces the albedo and hence the SW response.

Similar explanations apply for January (Figure 1, upper panel). In particular, note the January SW response at high NH latitudes. The peaked behavior is what one might expect because of the advance of January snow/ice cover relative to the annual mean.

Clouds significantly affect the TOA net (LW plus SW) response relative to a "clear sky" Earth, as is demonstrated in Figure 2 for both January and July. Because ΔR is the seasonal change in net upward radiation at the TOA, a cloud-induced reduction in ΔR causes radiative heating of the surface-atmosphere system. The cloudy versus clear response comparisons of Figure 2, for both January and July, thus show that seasonal cloud variations tend to produce radiative heating of the climate system, relative to the annual-mean climate, in the summer hemisphere together with cooling in the winter hemisphere. In the following section we provide more detail as to the mechanisms that produce this effect by examining $\Delta\text{CRF} = \Delta R_c - \Delta R$.

3.2. *Seasonal ΔCRF*

Seasonal ΔCRF and its LW and SW components are illustrated in Figure 3 for both January and July. Because the net ΔCRF acts to amplify both summer hemisphere heating and winter hemisphere cooling, it might be tempting to refer to this as a seasonal "positive cloud feedback." However, hemispheric changes cannot be used to infer cloud feedback, because they are largely dominated by seasonal variations of the ITCZ that are not related to cloud feedback, nor do we know how ΔCRF is partitioned between affecting the seasonal climate as opposed to oceanic storage and release of heat. It is important to reiterate the distinction between CRF and ΔCRF. In the present example of seasonal change, CRF is negative (cloud cooling) at mid-latitudes for both summer and the annual mean [*Harrison et al.*, 1990]. The fact that ΔCRF is positive during the summer at these latitudes means that seasonal cloud variations lessen this cooling; that is, they produce warming at summer midlatitudes relative to the annual mean.

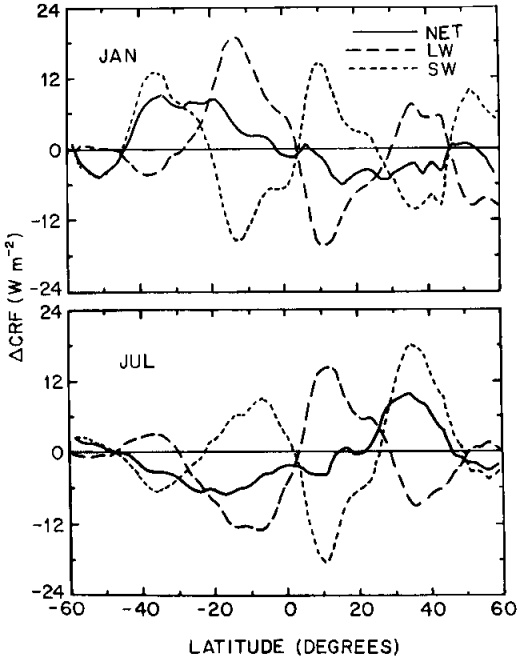

Fig. 3. Zonal-mean net, LW and SW ΔCRF for (upper panel) January and (lower panel) July.

There is substantial compensation between the LW and SW components of ΔCRF (Figure 3), particularly in the tropics where the large variation is again due to the ITCZ. Changes in CRF can be caused by changes in cloud amount, cloud vertical structure, cloud optical depth, and, in the present example, solar zenith angle. The effect due to cloud amount is clearly evident by the strong anticorrelation between the LW and SW components (Figure 3), since an increase in cloud amount will simultaneously increase the LW component and decrease the SW component. However, there are clearly other factors that contribute to ΔCRF.

To demonstrate this, we consider two regions having large positive ΔCRF for July as shown in Plate 1. Over the north Atlantic this is the consequence of a large positive SW component (not shown) that is moderated by a smaller negative LW component (Plate 2). This behavior is similar to the NH midlatitude zonal means (Figure 3), and it is partially the consequence of a winter to summer reduction in cloud cover; winter cloud cover is enhanced because of winter storm systems. Assuredly, however, there are related changes in cloud altitude and cloud optical depth. This is evident over southern China (Plate 1) where both the SW (not shown) and LW (Plate 2) components of ΔCRF are positive. Here there is substantial and comparable cloud cover in both winter and summer [*Stowe et al.*, 1989], but cloud altitude and cloud optical depth are quite different. In winter there is a predominance of stratus and stratocumulus, in contrast to a predominance of cirrus in summer; we expect cirrus optical depths to be much less than for stratus and stratocumulus. The increased height of the summer cirrus causes the July increase in LW ΔCRF shown in Plate 2, because an increase in cloud altitude enhances LW CRF [*Ramanathan*, 1989], while the related reduction in cloud optical depth, for cirrus relative to stratus and stratocumu-

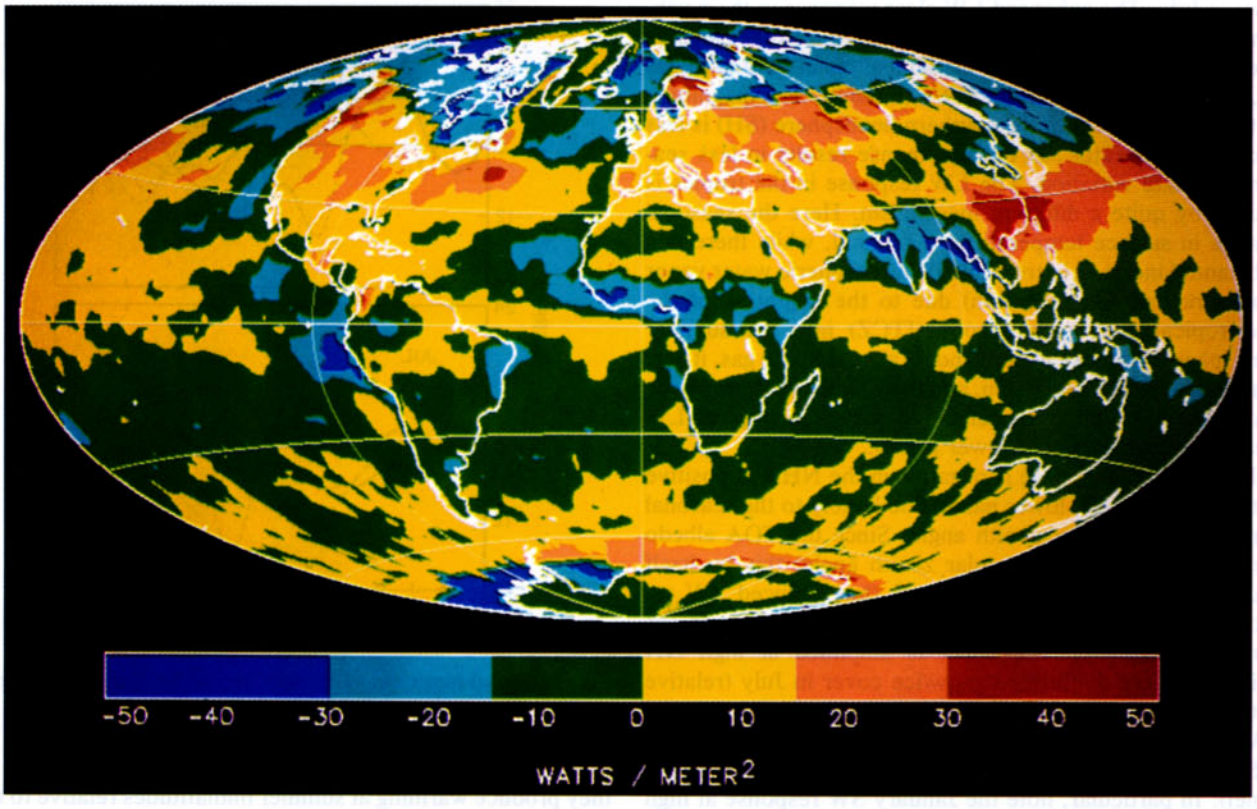

Plate 1. Geographical distribution of the net ΔCRF for July. For clarity, missing data in the four individual ERBE months have been filled by interpolation.

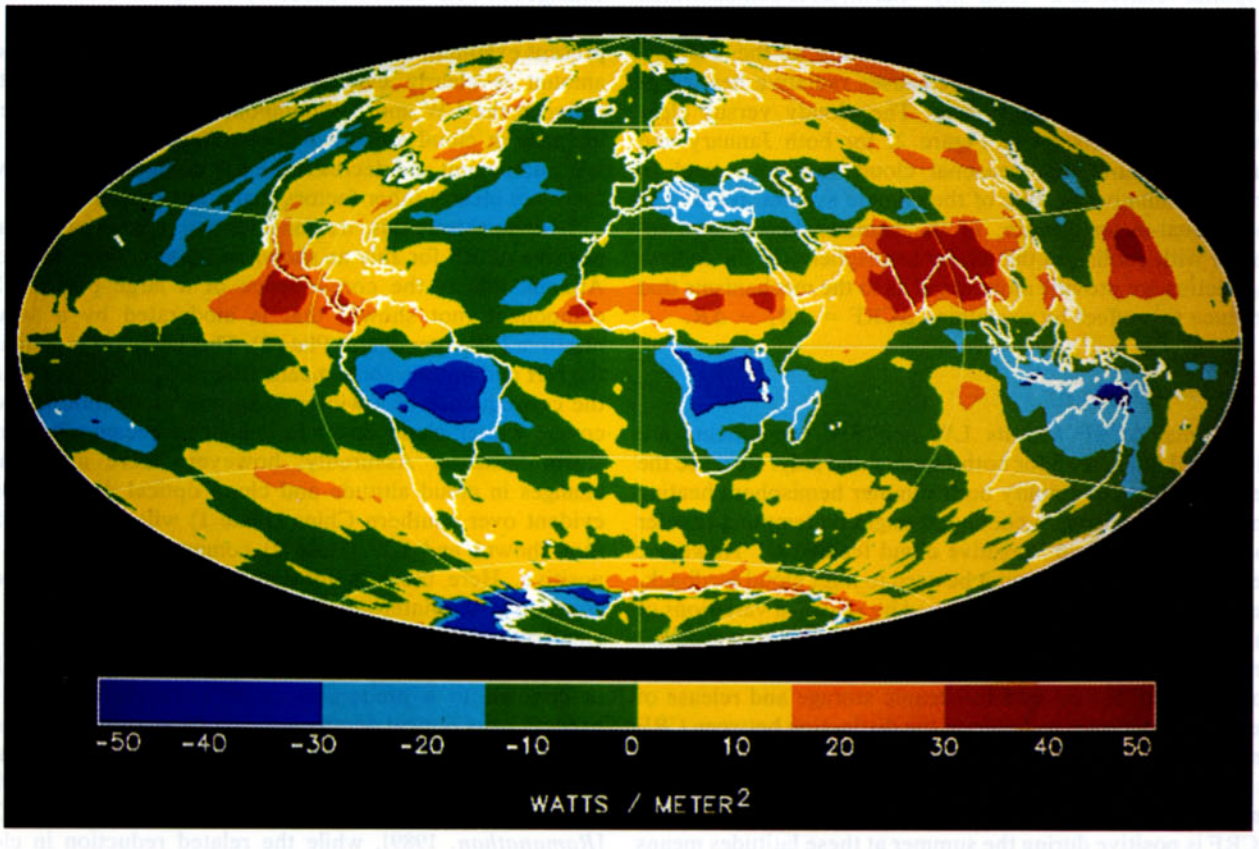

Plate 2. The same as in Plate 1 but for the LW component of ΔCRF.

lus, reduces the cloud albedo and thus increases the July SW ΔCRF by reducing the magnitude of the cooling. Thus while the northern Atlantic and southern China features appear similar in Plate 1, they are the consequence of quite different seasonal cloud changes as is evident from Plate 2.

4. CONCLUDING REMARKS

By separating clear from cloudy measurements the ERBE provides unique insights into seasonal variations of the Earth's climate system. In particular, this investigation proposes an approach for using such TOA radiation budget data for interpreting and understanding seasonal changes of cloud-radiative forcing in a manner that can serve as one means of testing GCMs. Specifically, the ERBE data demonstrate that, relative to the annual-mean climate, seasonal cloud variations produce radiative heating of the climate system in the summer hemisphere and cooling in the winter hemisphere. In view of the disagreements among 19 atmospheric GCMs [*Cess et al.*, 1990] concerning climate-induced changes in CRF, these data are an important and timely resource to help improve the simulation of cloud-climate interactions in GCMs.

Acknowledgments. This work was supported by the National Aeronautics and Space Administration through the ERBE Project and by the National Science Foundation through grant ATM-8815885.

REFERENCES

Cess, R. D., et al., Interpretation of cloud-climate feedback as produced by 14 general circulation models, *Science*, *245*, 513–516, 1989.

Cess, R. D., et al., Intercomparison and interpretation of climate feedback processes in 19 atmospheric general circulation models, *J. Geophys. Res.*, *95*, 16,601–16,615, 1990.

Harrison, E. F., P. Minnis, B. R. Barkstrom, V. Ramanathan, R. D. Cess, and G. G. Gibson, Seasonal variation of cloud radiative forcing derived from the Earth Radiation Budget Experiment, *J. Geophys. Res.*, *95*, 18,687–18,703, 1990.

Ramanathan, V., R. D. Cess, E. F. Harrison, P. Minnis, B. R. Barkstrom, E. Ahmad, and D. Hartmann, Cloud-radiative forcing and climate: Results from the Earth Radiation Budget Experiment, *Science*, *243*, 57–63, 1989.

Randall, D. A., and S. Tjemkes, Clouds, the Earths radiation budget, and the hydrologic cycle, *Paleoecology*, *90*, 3–9, 1991.

Stowe, L. L., H. Y. M. Yeh, T. F. Eck, C. G. Wellemeyer, H. L. Kyle, and the Nimbus-7 Science Team, Nimbus-7 global cloud climatology. Part II, First year results, *J. Climate*, *2*, 671–709, 1989.

B. R. Barkstrom, E. F. Harrison, and P. Minnis, Atmospheric Sciences Division, NASA Langley Research Center, Hampton, VA 26665.

R. D. Cess and T. Y. Kwon, Institute for Terrestrial and Planetary Atmospheres, State University of New York, Stony Brook, NY 11794.

V. Ramanathan, Scripps Institution of Oceanography and California Space Institute, University of California at San Diego, La Jolla, CA 92093.

(Received June 14, 1991;
revised January 30, 1992;
accepted January 31, 1992.)